Available online at www.sciencedirect.com
SCIENCE DIRECT®
Carbohydrate Polymers 56 (2004) 447–458
Carbohydrate Polymers
www.elsevier.com/locate/carbpol

Amylose–lipid complexation: a new fractionation method

G.G. Gelders*, T.C. Vanderstukken, H. Goesaert, J.A. Delcour

Laboratory of Food Chemistry, Katholieke Universiteit Leuven, Kasteelpark Arenberg 20, B-3001 Leuven, Belgium

Received 22 January 2004; accepted 18 March 2004

Available online 14 May 2004

Abstract

Amylose fractions of different peak Degree of Polymerisation (DP) (DP20, DP60, DP400, DP950) were complexed with docosanoic acid (C22) and glyceryl monostearate (GMS) at 60 and 90 °C. Complexation yields, relative crystallinities, dissociation temperatures and enthalpies increased with amylose chain lengths (DP20–DP60–DP400). Relative crystallinities and thermal stabilities of the DP950-complexes were slightly lower than those of the other amylose fractions, probably due to increased conformational disorders, resulting in crystal defaults. Molecular weight distributions of the complexes revealed that, irrespective to the complexation temperature, the critical DP for complex formation and precipitation was 35 and 40 for complexes with GMS and C22, respectively, corresponding to the length needed to accommodate two GMS- or C22-molecules within an amylose helix. Complexation of dextrins with a well-chosen lipid, allows to separate starch derived dextrins with a predictable critical chain length as border. Dextrins, of sufficient DP will complex and precipitate, while the shorter dextrins will remain in solution.

Keywords: Complexation; V-amylose; Chain length; High-performance anion-exchange chromatography with pulsed amperometric detection; Size-exclusion chromatography; Fractionation

1. Introduction

Amylose, the essentially linear α-D-(1 → 4)-glucopolymer of starch, has the unique feature to form helical inclusion complexes with several organic and inorganic complexing agents. Indeed, in contrast to other glucopolymers, like dextran [α-D-(1 → 6)-bonds] or cellulose [β-D-(1 → 4)-bonds], amylose chains have a gradual natural twist which makes a helicoidal conformation possible and unique (Zobel, 1988). Complexing agents such as iodine, dimethylsulfoxide (DMSO), lipids, alcohols, flavour compounds, etc. induce the formation of single, left-handed amylose helices with a pitch of 0.805 nm, also known as V-amylose (Buléon, Colonna, Planchot, & Ball, 1998). The inner diameter (0.48, 0.63 and 0.78 nm) is controlled by the size of the complexing agent, resulting in helices with 6 (lipids, linear alcohols), 7 (branched chain alkyl compounds) or 8 (more bulky compounds) glucose residues-per-turn (Rappenecker & Zugenmaier, 1981; Rutschmann & Solms, 1990; Takeo, Tokumura, & Kuge, 1973). The glucosyl hydroxyl groups are located at the outer surface of the helix, while the inner surface is lined with methylene groups and glycosidic oxygens resulting in a more hydrophobic cavity, similar to that of cyclodextrins (Immel & Lichtenthaler, 2000; Whittam et al., 1989). Consecutive turns of helices are stabilised by numerous intra- and interhelical van der Waals contacts and hydrogen bonds (Rappenecker & Zugenmaier, 1981). However, the driving force for complex formation is presumably of hydrophobic nature and involves transfer of the hydrophobic guest molecule from water to the less polar environment within the amylose helix (Fanta, Shogren, & Salch, 1999; Krog, 1971; Kubik & Wulff, 1993; Whittam et al., 1989). The best-known inclusion complexes are amylose–lipid complexes, naturally present in starch and/or formed during gelatinisation with endogeneous or added lipids (Morrison, Tester, Snape, Law, & Gidley, 1993). Their importance is reflected in numerous food applications, such as the use of emulsifiers to retard bread staling (Riisom, Krog, & Eriksen, 1984). Today, other fields of science, such as nanotechnology [helical wrapping of carbon nanotubes (Lii, Stobinski, Tomasik, & Liao, 2003; Star, Steuerman, Heath, & Stoddart, 2002)] and biotechnology [artificial chaperoning of proteins (Sundari, Raman, & Balasubramanian, 1999) and chiral separation

* Corresponding author. Tel.: +32-16-32-16-34; fax: +32-16-32-19-97.
E-mail address: greet.gelders@agr.kuleuven.ac.be (G.G. Gelders).

0144-8617/$ - see front matter © 2004 Elsevier Ltd. All rights reserved.
doi:10.1016/j.carbpol.2004.03.012

of pharmaceuticals (D'Hulst & Verbeke, 1996)] begin to exploit the amylose-complexing abilities.

The polar carboxyl and glycerol groups of fatty acids and monoacylglycerols, respectively, do not enter the hydrophobic cavity because of steric and/or electrostatic repulsions (Carlson, Larsson, Dinh-Nguyen, & Krog, 1979; Godet, Tran, Delage, & Buléon, 1993a; Snape, Morrison, Maroto-Valer, Karkalas, & Pethrick, 1998). This limits helical segment lengths to two fatty acids or monoacylglycerol molecules situated with their terminal methyl groups end-to-end (Godet, Bizot, & Buléon, 1995a; Godet, Bouchet, Colonna, Gallant, & Buléon, 1996).

Molecular association of amylose and lipids is, under suitable conditions, followed by crystallisation. At low complexation temperatures (≤ 60 °C), the nucleation rate is very high and amylose helices 'freeze' rapidly in a structure with little crystallographic order. Due to the random distribution of helices, no distinct crystallites exist. This kind of 'amorphous' or 'type I' amylose–lipid complex has a low (< 100 °C) dissociation temperature. In contrast, higher complexation temperatures (≥ 90 °C) yield 'semi-crystalline' or 'type II' amylose–lipid complexes because slow nucleation is followed by distinct crystal growth (Biliaderis & Galloway, 1989). A distinction is made between type II_a and II_b amylose–lipid complexes based on the degree of crystallinity and/or perfection of the ordered domains. Type II_b complexes have a slightly higher melting temperature than type II_a complexes but both are above 100 °C (Seneviratne & Biliaderis, 1991).

In the past, several studies dealt with the influence of the nature of lipids on the complexation with (potato) amylose. Complexation was performed at 60 and at 90 °C to promote types I and II complexes, respectively. Godet, Buléon, Tran, and Colonna (1993b), Godet et al. (1995a), Godet, Tran, Colanna, Buléon and Pezolet (1995b) and Godet et al. (1996) focused on the influence of amylose Degree of Polymerisation (DP) (DP30, DP40, DP80 and DP900) on the complexation with short (C8–C10–C16) fatty acids at a complexation temperature of 90 °C. A lamellar-like (alternation of crystalline and amorphous areas) morphology of the crystals has been described with a crystal thickness strongly depending on DP (Godet et al., 1996). However, the minimum amylose DP, necessary to form a complex (type I or II) with a monoacylglycerol and a long fatty acid and to precipitate from the complexation medium has not been determined, and, to the best of our knowledge, neither has the influence of complexation temperature on the formation of types I and II amylose–lipid complexes with lower amylose DPs.

In the present study, amyloses of different peak DP (20, 60, 400, 950) were complexed with a fatty acid (docosanoic acid; C22) and a monoacylglycerol (glyceryl monostearate; GMS) at 60 and at 90 °C and the resulting complexes were characterised. This was done to elucidate the critical DP required for complex formation on the one hand and on the other hand, the minimal DP necessary to obtain type II complexes. Moreover, the possibility to fractionate dextrin populations by complexation with lipids was evaluated.

2. Experimental

2.1. Materials

2.1.1. Amyloses and lipids

Four amylose fractions, with different peak DP (determined as described below), were prepared from different starch sources (Fig. 1). Potato amylose (peak DP950) was purchased from Serva Feinbiochemica (Heidelberg, Germany). A portion of this material (40 g) was degraded with barley β-amylase [2 mg/l] (A-7130, Sigma-Aldrich, Bornem, Belgium) at pH 4.8 and 37 °C during 60 min as described by Eerlingen, Deceuninck, and Delcour (1993) resulting in the second amylose fraction, with peak DP400. Amylose of peak DP60 was obtained after hydrolysis at pH 5.0 by a thermostable α-amylase (1 h at 100 °C) and an amyloglucosidase (24 h at 60 °C) of retrograded high-amylose maize starch [Novelose 330 (National Starch

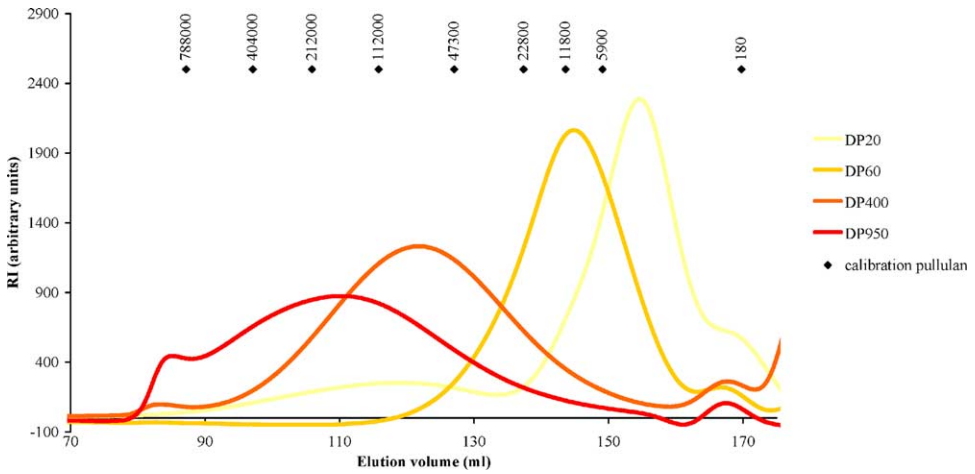

Fig. 1. Sephacryl S-400 HR size-exclusion chromatograms of amylose fractions with DP20, 60, 400 and 950 (showing the refractive index signal).

and Chemical Company, Bridgewater, NJ, USA)] as described by Andersson, Rydberg, Larsson, Andersson, and Åman (2002). The fourth amylose fraction (peak DP20) was obtained by debranching waxy maize starch [Meritena 300 (Amylum N.V., Aalst, Belgium)] with Promozym 800 (Novo Nordisk, Bagsvaerd, Denmark) according to Dutch patent 7001026 (Hayashibare Company, 1970). All amylose fractions were defatted prior to complexation with 85% methanol for 24 h in a Soxhlet extractor.

Lipids used were docosanoic acid (C22), purchased from Acros Organics (Geel, Belgium), and Dimodan PVP (glyceryl monostearate, GMS) (purity >90%), kindly donated by Danisco (Brabrand, Denmark). All other reagents were of at least analytical grade and supplied by Sigma-Aldrich (Bornem, Belgium).

2.2. Methods

2.2.1. Determination of molecular weight and polydispersity

The (peak) DP values of the amylose fractions and amylose–lipid complexes (Section 2.2.2) were determined with Size-Exclusion Chromatography (SEC) on a Sephacryl S-400 HR (fractionation range 1×10^4–2×10^6 M_r dextran; 100 cm × 1.6 cm) or a Superose 12TM column (fractionation range 1×10^3–3×10^5 M_r globular proteins; 30×1 cm^2) (Amersham Biosciences, Uppsala, Sweden). Both columns were calibrated with Shodex P-82 pullulan standards (Showa Denko, Japan), maltoheptaose and glucose (Sigma-Aldrich, Bornem, Belgium). It was found by Roger, Axelos, and Colonna (2000) that pullulans can be used to replace linear amylose standards for chromatographic calibration purposes when 0.1 M potassium hydroxide is used as solvent. A second order polynomial correlation was found between the logarithm (M_r standards) and the elution volume. Each eluted peak was characterised by the peak DP (= M_r/162). It is this DP value which is used in the present paper. The polydispersity (P) was estimated for each amylose fraction and corresponding complexes, based on the above mentioned pullulan calibration. P is defined as the ratio of the weight average DP (DP_w) to the number average DP (DP_n) with

$$DP_w = \frac{\sum_{i=1}^{\infty} DP_i m_i}{\sum_{i=1}^{\infty} m_i} \text{ and } DP_n = \frac{\sum_{i=1}^{\infty} DP_i (m_i/M_i)}{\sum_{i=1}^{\infty} (m_i/M_i)}$$

with m_i the mass concentration and M_i the molecular weight of amylose chains with a DP = i.

A Biologic Duo Flow Core System (Bio-Rad Laboratories, Hercules, CA, USA) equipped with a Signal Import Module-HR (SIM-HR) and a RID-10A Detector (Shimadzu, Kyoto, Japan) was used. Samples [15 mg (Sephacryl S-400 HR) or 25 mg (Superose 12TM)] were solubilised for at least 12 h in 1.0 M potassium hydroxide under mild magnetic stirring and then diluted with 9 volumes of water. After filtration (0.45 μm; regenerated cellulose syringe filter), 100 μl (Superose 12TM) or 5 ml (Sephacryl S-400 HR) of the solubilised samples were injected.

Elution was with 0.1 M potassium hydroxide (containing 0.02% sodium azide) at a flow rate of 0.5 ml/min and at ambient temperature.

2.2.2. Amylose–lipid complexation

Solution-grown amylose–lipid complexes were prepared in a DMSO–water mixture (1:15) at 60 or 90 °C based on Galloway, Biliaderis, and Stanley (1989). Each amylose fraction (4.0 g) was dissolved in 25 ml hot DMSO and diluted with 375 ml boiling water. The resulting solutions (1.0%, w/v) were boiled for 30 min and equilibrated in a water bath at 60 or 90 °C. C22 or GMS (0.8 g), dissolved in 20 ml hot ethanol (weight ratio of amylose to lipid 5:1), was then slowly added to the solution under vigorous mixing. The complexes were isothermally grown for 4 h with gentle stirring every half hour. The mixture was then slowly cooled (12 h) to ambient temperature. For each amylose fraction, a control was prepared at 60 or 90 °C with the same procedure, but with addition of hot ethanol without lipid.

The 16 complexes, labelled with the following information-bearing codes 'DP of amylose fraction–lipid-complexation temperature' (e.g. DP950-GMS-60 °C) and eight controls, labelled, e.g. as DP950-60 °C, were recovered by centrifugation (10,000g, 6 °C, 30 min). Supernatants were decanted and residues washed with 200 ml water, centrifuged (10,000g, 6 °C, 15 min) and freeze-dried. Complexes were gently powdered (250 μm) and suspended (30 min) in chloroform (60 ml/g complex) at ambient temperature to remove excess free lipid. The complex suspensions were filtered over a crucible with a sintered glass filter (porosity 4) and thoroughly washed with chloroform. The chloroform washed complexes were air-dried.

2.2.3. Determination of complexation yield

The complexation yield (CY) was defined as the ratio of the number of moles of complexed and chloroform washed amylose recovered to the initial total number of moles amylose and expressed in percentages. This required determination of the composition of the complexes. Total glucose content of complexes and amylose fractions was determined by acid hydrolysis followed by reduction, acetylation and gas chromatographic determination of the resulting sorbitol acetate. (Englyst & Cummings, 1984). The samples were separated on a Supelco SP-2380 polar column (30 m × 0.32 mm i.d., 0.2 μm film thickness, Supelco, Bellefonte, PA, USA) in an Agilent chromatograph (Agilent 6890 series, Wilmington, DE, USA) equipped with an autosampler, a splitter injection port (split ratio = 1:20), and a flame ionisation detector. The inlet and detector temperatures were 270 °C, while separation took place at 225 °C. The carrier gas was helium. The coefficient of variation, defined as the ratio of the standard deviation and the mean of the obtained results was less than 5%.

2.2.4. X-ray diffraction and determination of relative crystallinity

Wide angle X-ray diffraction measurements were performed with Ni-filtered Cu K_α radiation on a Rigaku rotating anode device (Manners, USA) operating at 40 kV and 100 mA, using a Rigaku high temperature X-ray diffractometer (Manners, USA). Detection was with a scintillation counter with a powder diffractometer operated in transmittance. Samples (moisture ca. 10%) were sealed between two pieces of aluminium tin foil. The scanning rate was 10 s per step of 0.05° 2θ over a range of 3–33° 2θ. Amorphous waxy maize starch was prepared in a rotating flask by heating an aqueous starch suspension (2.0%, w/v) at 85 °C for 20 min. The dilute paste was then boiled (100 °C) for 1 h. The sample was frozen with liquid nitrogen and freeze-dried. Diffraction patterns of amylose–lipid complexes and the amorphous sample were normalised to the total diffused intensity between 6 and 30° 2θ. The normalised amorphous diffraction pattern was fitted to the main minima of the normalised amylose–lipid complex diffraction pattern. The relative crystallinity (X_c) between 6 and 30° 2θ was calculated using the formula

$$X_c = \frac{(S_{sample} - S_{amorphous})}{S_{sample}}$$

with S_{sample} integrated intensity of normalised amylose–lipid complex diffraction pattern; $S_{amorphous}$ integrated intensity corresponding to the fitted amorphous sample.

2.2.5. DSC

Differential scanning calorimetry (DSC) was performed with a Seiko DSC 120 (Kawasaki Kanagawa, Japan). Samples (2–4 mg) were accurately weighed into coated aluminium sample pans and water was added (1:3 w/w sample dm/water). The pans were sealed, weighed and equilibrated overnight at room temperature to distribute the water evenly in the sample. After checking pan weight for possible moisture loss, the sample pan and an empty reference pan were heated from 30 to 135 °C at 4 °C/min. Calibration was with indium and tin. Onset (T_0), peak (T_m), conclusion (T_c) (dissociation) temperatures and enthalpies (ΔH) of amylose–lipid complexes were determined with Seiko software. ΔH was expressed as J/g complex dry matter and temperatures in °C. Results were averages of at least three measurements. The coefficient of variation, defined as the ratio of the standard deviation and the mean of the obtained results was less than 1.5% for T_m. For ΔH values, respective standard deviations are given.

2.2.6. High-performance anion-exchange chromatography with pulsed amperometric detection

High-performance anion-exchange chromatography with pulsed amperometric detection (HPAEC-PAD) was performed with a Dionex DX-500 chromatography system (Sunnyvale, CA, USA) equipped with an ED-40 electrochemical detector, a GP-40 gradient pump and an AS-3500 autosampler. Samples (10 mg) were solubilised in 1.0 ml hot DMSO and placed in a water bath at 100 °C for 10 min. Hot water (1.0 ml) was added and the mixed samples were boiled for another 10 min. The filtered (0.25 μm; regenerated cellulose syringe filters) samples were injected (25 μl) onto a CarboPac PA-100 anion-exchange column (250 mm × 4 mm) in combination with a CarboPac PA-100 guard column. The pulse potentials and durations, the eluents and the eluent gradient programme were as described by Gelders, Bijnens, Loosveld, Vidts, and Delcour (2003).

3. Results and discussion

3.1. Amylose–lipid complexation

Table 1 lists the CY for all amylose fractions complexed with GMS or C22 at 60 and at 90 °C. CY increased with DP regardless of complexation temperature and lipid type. According to Godet, Bizot, and Buléon, (1995a), this behaviour is the net result of amylose solubility and the ability of the amylose and the lipid to form complexes and precipitate in the complexation medium. The DMSO–water (1:15) complexation medium is a good solvent for the shortest amylose (DP20). Only 5 and 8% of the dissolved DP20 precipitated in the control complexation (without lipid) at 60 and 90 °C, respectively. Yields of the other amylose controls ranged between 58 and 73%. All the amylose controls had weak B-type amylose X-ray diffractograms, typical for retrograded amylose. The complexation temperature apparently did not influence the CY. However, CY of GMS complexes were higher than those of the respective C22 complexes, in particular for the low DP amyloses (DP20 and DP60). A possible explanation is based on the number of glucose molecules surrounding the lipid guest molecules. The length of a GMS molecule without the glycerol group and of a C22 acid without the carboxyl group are 2.27 and 2.77 nm, respectively (Karkalas & Raphaelides, 1986). When lipids are positioned with their methyl groups end-tot-end within the amylose helix as postulated by Godet et al. (1995a, 1996), the helical segment length would be limited to roughly 4.54 and 5.54 nm, respectively. With a pitch of 0.805 nm and six glucose molecules per helix-turn, this corresponds to amylose DPs of 34 and 41,

Table 1
Complexation yield, CY (%), of amylose (DP20, 60, 400 or 950) complexed with glyceryl monostearate (GMS) or docosanoic acid (C22) at 60 or at 90 °C

Amylose	GMS		C22	
	60 °C	90 °C	60 °C	90 °C
DP20	28.7	31.4	4.5	4.5
DP60	87.9	84.9	37.8	40.5
DP400	98.3	95.7	83.5	76.6
DP950	100.0	100.0	100.0	97.9

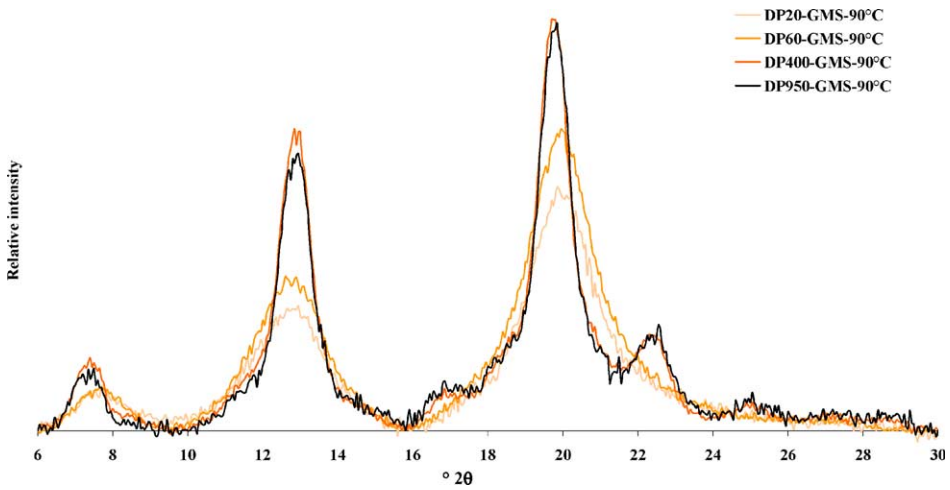

Fig. 2. Normalised V-type X-ray diffractograms of amylose (DP20, DP60, DP400, DP950)-GMS complexes formed at 90 °C.

required for complex formation with GMS and C22, respectively. The abundancy of dextrins with DP > 41 in amylose fractions DP20 and DP60 is much smaller than that of dextrins with DP > 34 (Fig. 1). This explains the smaller CY of DP20- or DP60-C22 complexes than that of the corresponding DP20- or DP60-GMS complexes. However, this explanation is not valid for the higher DP amylose fractions tested (DP400 and DP950) because they contain only negligible amounts of DP < 41. Moreover, one has to take into account that the applied experimental conditions are not the most favourable for fatty acids, as reported by Karkalas, Ma, Morrison, and Pethrik (1995). Complexation with fatty acids in warm alkaline solution (pH ~ 12) has distinct advantages. The interaction of the soluble monomeric potassium salt with amylose eliminates co-precipitation of uncomplexed fatty acids and excludes the risk of forming double-helical retrograded amylose (Raphaelides & Karkalas, 1988). In addition, whereas amylose–monoacylglycerol complexes precipitate spontaneously in neutral aqueous media, insoluble amylose–fatty acid complexes are more efficiently obtained at pH ~ 5 (Karkalas et al., 1995).

3.2. Relative crystallinity

All amylose fractions showed an X-ray diffraction profile characteristic of the B-type amylose (results not shown) whereas all complexes, even those formed at 60 °C, showed a clear V-amylose diffractogram with main reflections at Bragg angles 7.36, 13.1 and 20.1° 2θ. For the longest amylose chain lengths (DP400 and DP950), minor reflections at Bragg angles 17 and 22.5° 2θ were observed and the main diffraction peaks became sharper (Fig. 2). Knowing that all amylose controls (without lipid) resulted in a (weak) B-pattern, we can conclude that addition of GMS or C22 to dissolved amylose changed the conformation of all amylose fractions, even the DP20 fraction, indicating complex formation. It is surprising that the complexes formed at 60 °C, which in literature are described as amorphous (Biliaderis & Galloway, 1989), also resulted in semi-crystalline V-patterns. However, when a wet pellet of DP20-GMS-60 °C complex was analysed, it only showed a very weak V-pattern. Indeed, the drying procedure of the complexes has an important impact on their structure (Nuessli, Putaux, Le Bail, & Buléon, 2003). According to Biliaderis and Seneviratne (1990) freeze-drying modifies the structure of type I complexes by formation of chain aggregates of a much higher order. However, DSC parameters of type I complexes are not altered by freeze-drying (Biliaderis & Seneviratne, 1990).

Relative crystallinity increased with increasing amylose DP (Table 2). The longer amylose fractions (DP60, DP400) yielded inclusion complexes with improved crystalline features and larger crystallite size (Godet et al., 1996). The DP950-complexes had slightly lower relative crystallinity. This was probably due to increased conformational disorders, which are more likely to be formed for the longest amylose DPs and result in crystal defaults (Godet et al., 1995b). Relative crystallinities of complexes formed at 60 and at 90 °C did not differ a lot for DP20 and DP60 fractions. Only for the longest amylose chain lengths (DP400 and DP950), the difference in relative crystallinity increased when complexes were formed at 60 and at 90 °C. In our view, DP20 and DP60 amyloses are too short to organize themselves in a lamellar-like morphology, either in

Table 2
Relative crystallinity (%) of amylose–lipid complexes; obtained with amylose (DP20, 60, 400, 950) complexed with glyceryl monostearate (GMS) or docosanoic acid (C22) at 60 or at 90 °C

Amylose	GMS		C22	
	60 °C	90 °C	60 °C	90 °C
DP20	58.0	61.0	46.9	48.6
DP60	71.4	72.2	71.3	73.2
DP400	75.9	82.7	78.9	77.3
DP950	72.3	82.7	68.6	74.7

Table 3
Dissociation temperatures, T_m (°C) and enthalpies, ΔH (J/g dm) of chloroform washed complexes produced from amylose (DP20, 60, 400 or 950) and glyceryl monostearate (GMS) or docosanoic acid (C22) at 60 or at 90 °C

Amylose		**GMS**					**C22**			
		60 °C		90 °C			60 °C		90 °C	
		T_m (°C)	ΔH (J/g dm)	T_m (°C)	ΔH (J/g dm)		T_m (°C)	ΔH (J/g dm)	T_m (°C)	ΔH (J/g dm)
DP20	FL	51.96	0.18 (0.04)	–	–	FL	79.33	1.60 (0.66)	77.07	17.33 (7.82)
	I	85.98 97.32	11.67 (1.34)	86.60 99.97	13.03 (0.64)	I	84.80 100.00	1.20 (0.20)	87.93 102.67	3.07 (1.12)
	II	–	–	119.10	0.20 (0.14)	II	–	–	–	–
DP60	FL	–	–	–	–	FL	74.75	0.90 (0.00)	74.37	0.20 (0.00)
	I	92.43	18.83 (0.84)	90.67	19.67 (1.00)	I	97.03	20.90 (0.75)	96.17	23.43 (2.19)
	II	–	–	110.37 115.23	2.30 (0.10)	II	–	–	–	–
DP400	FL	–	–	–	–	FL	–	–	–	–
	I	96.70	32.93 (1.92)	96.25	− 1.00 (0.29)	I	104.80	24.15 (2.98)	103.40	11.63 (1.19)
	II	119.73	0.90 (0.28)	114.72 121.43	23.27 (6.25)	II	106.88			
							–	–	117.89 121.40 126.75	15.44 (4.37)
DP950	FL	–	–	–	–	FL	–	–	76.72	0.20 (0.00)
	I	97.50	24.47 (1.66)	–	–	I	102.80	26.15 (1.34)	104.43	19.73 (0.91)
	II	–	–	113.10 121.35	26.2 (4.40)	II	–	–	120.17	7.27 (0.55)

Abbreviations. FL, free lipid; I, type I complex; II, type II complex. Standard deviation enthalpy between brackets.

a fringed micellar organization or by folding at the surface of the crystallites in the same crystalline lamella. Therefore, we suggest that no distinction can be made between a type I and II complex for such amyloses.

3.3. Thermal stability

Prior to washing with chloroform, all complexes had a low-temperature DSC transition, caused by melting of free GMS ($T_m = 52.9\,^{\circ}C$) or free C22 ($T_m = 75.8\,^{\circ}C$) (results not shown). For each amylose chain length, GMS or C22 was therefore present in excess and saturation of the amylose fractions was possible under the complexation conditions used. The ΔH of the free lipid was the highest for DP20-complexes and decreased gradually to a minimum value of circa 7 J/g dm for the DP950-complexes. This is a logical trend, because less lipid is required to saturate shorter amyloses.

Washing with chloroform removed only non-complexed lipid, as ΔH values of the complexes remained the same or

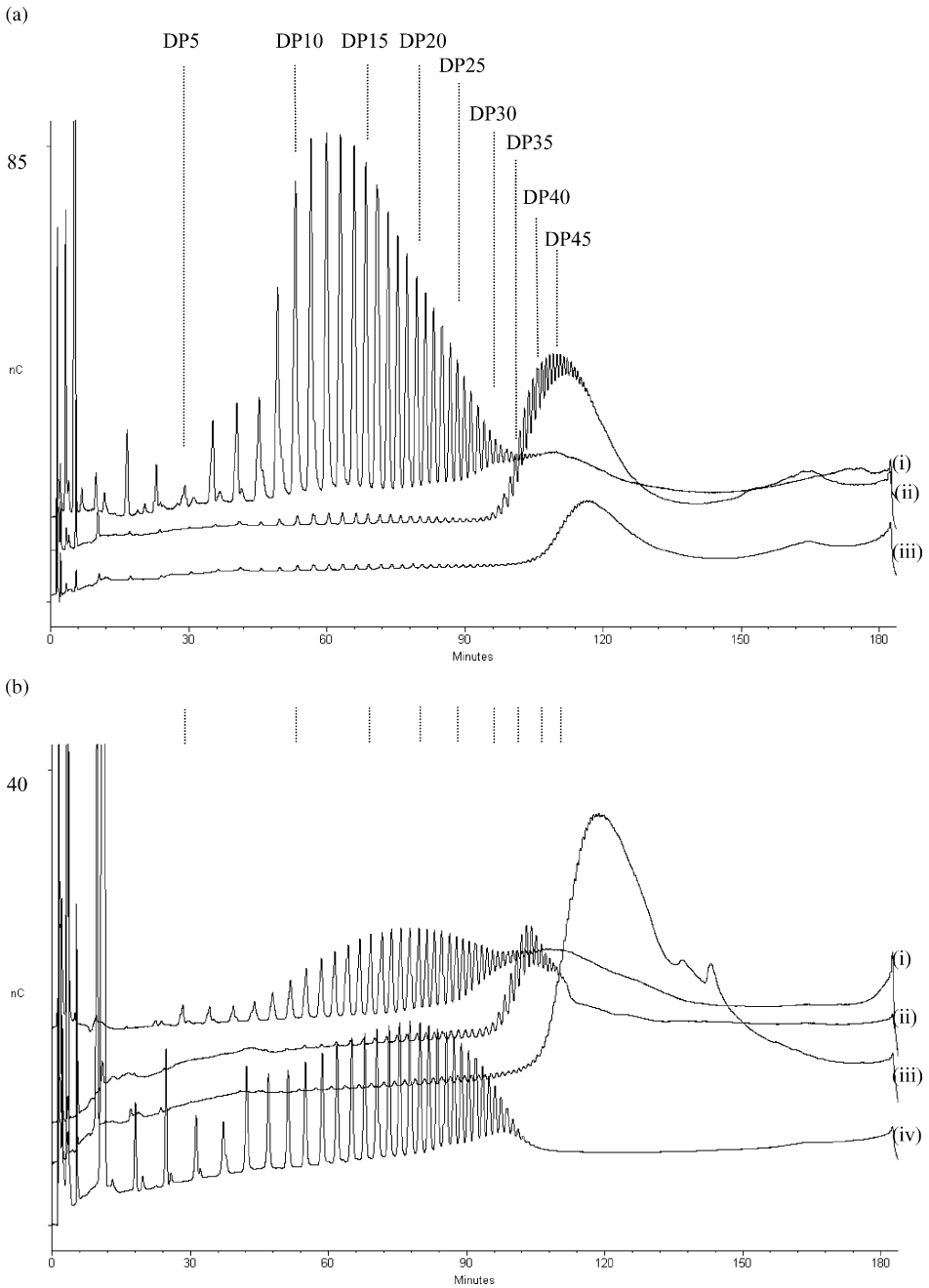

Fig. 3. High-performance anion-exchange chromatography with pulsed amperometric detection (HPAEC-PAD) profiles of (a) DP20 and its complexes formed at 90 °C: (i) DP20; (ii) DP20-GMS-90 °C; (iii) DP20-C22-90 °C and of (b) DP60 and its complexes formed at 90 °C: (i) DP60; (ii) DP60-GMS-90 °C; (iii) DP60-C22-90 °C; (iv) supernatant of DP60-GMS-90 °C.

even increased a little due to concentration effects. Table 3 reveals that only for some C22-complexes traces of free lipid were observed and that the chloroform washing was successful. T_m of the complexes increased with increasing DP because of improved crystalline features of the complexes, in particular crystallite size. T_m of the DP950-complexes were only slightly higher (or even somewhat lower) than those of the DP400-complexes. This could be expected, given the relative crystallinities of these complexes (Table 2). Comparison of GMS-complexes formed at 60 and at 90 °C shows that, for amylose fractions DP20 and DP60, predominantly type I complexes were

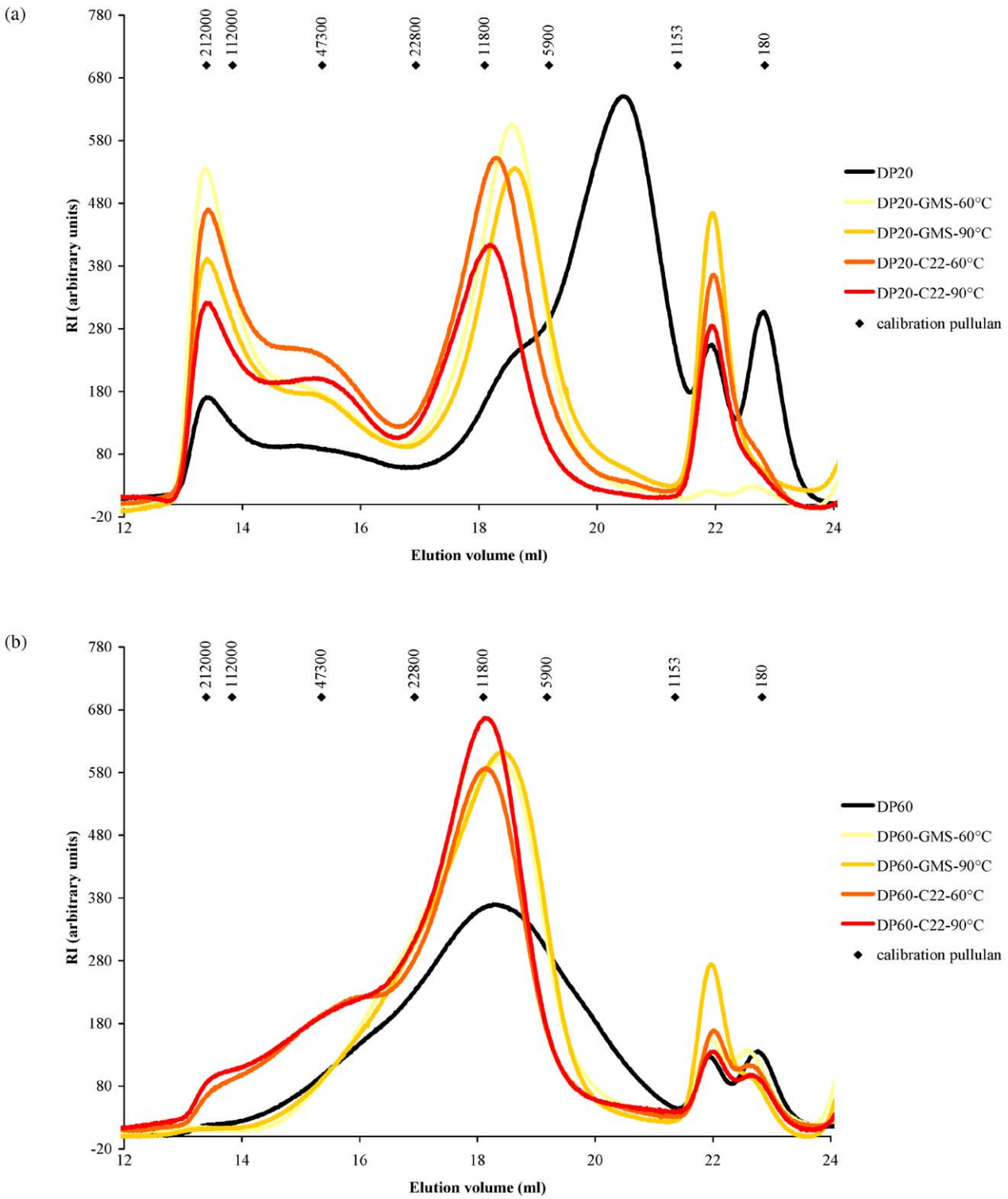

Fig. 4. Superose 12TM size-exclusion chromatograms of (a) DP20 and its complexes and of (b) DP60 and its complexes (showing the refractive index signal).

Table 4
Weight (DP_w) and number (DP_n) average degree of polymerisation and polydispersity (P) for each amylose fraction and the corresponding complexes, calculated by means of a pullulan calibration curve specific for Superose 12 TM column (DP20 and DP60) and Sephacryl S-400 column (DP400 and DP950)

Amylose/complex	DP_w	DP_n	P
DP20	122.5	22.2	5.5
DP20-GMS-60 °C	289.1	74.1	3.9
DP20-GMS-90 °C	265.6	63.1	4.2
DP20-C22-60 °C	296.3	82.3	3.6
DP20-C22-90 °C	296.2	93.7	3.2
DP60	165.7	71.2	2.3
DP60-GMS-60 °C	156.6	87.0	1.8
DP60-GMS-90 °C	152.5	86.7	1.8
DP60-C22-60 °C	226.8	120.1	1.9
DP60-C22-90 °C	199.2	103.0	1.9
DP400	535.3	171.7	3.1
DP400-GMS-60 °C	509.3	187.0	2.7
DP400-GMS-90 °C	453.0	180.8	2.5
DP400-C22-60 °C	496.1	182.1	2.7
DP400-C22-90 °C	299.3	158.6	1.9
DP950	1374.4	492.2	2.8
DP950-GMS-60 °C	1384.5	525.7	2.6
DP950-GMS-90 °C	1173.3	476.3	2.5
DP950-C22-60 °C	933.9	406.2	2.3
DP950-C22-90 °C	1279.0	488.0	2.6

obtained. Complexes with DP400 and DP950 amylose were more of type II when formed at 90 °C than when formed at 60 °C. The same trends were observed for the C22-complexes, although less clearly for the DP400 and DP950-C22 complexes where a mixture of both types I and II complexes were obtained. These data indicate that an amylose DP exceeding 60 is required for formation of type II complexes. Furthermore, higher T_m were observed for the C22-complexes than for the corresponding GMS-complexes. This was expected based on the larger helical chain length in the crystallites for C22-complexes.

The total ΔH for complex mixtures (sum of ΔH values where both types I and II were present) increased with increasing amylose DP. In contrast, Godet et al. (1995a) reported ΔH to decrease with amylose DP. In addition, only a small difference in total ΔH between complexes formed at 60 or at 90 °C was noted. When trying to explain these observations, we came across ambiguous information in literature. Biliaderis and Galloway (1989)—based on their work and that by Kowblansky (1985)—believe that the same stabilizing forces are involved in types I and II complexes, resulting in similar ΔH values, and that differences between the two types are mainly entropic ($T_m = \Delta H/\Delta S$). Biliaderis and Seneviratne (1990) consider the interchain packing energy to be almost negligible when compared to the total ΔH of dissociation, solvation and uncoiling. In contrast, Karkalas et al. (1995) claimed that ΔH values for type II complexes are significantly higher than those for type I complexes. In the latter view, the ΔH difference is attributed to the net dissociation energy of the numerous van der Waals contacts between helices and limited interhelical hydrogen

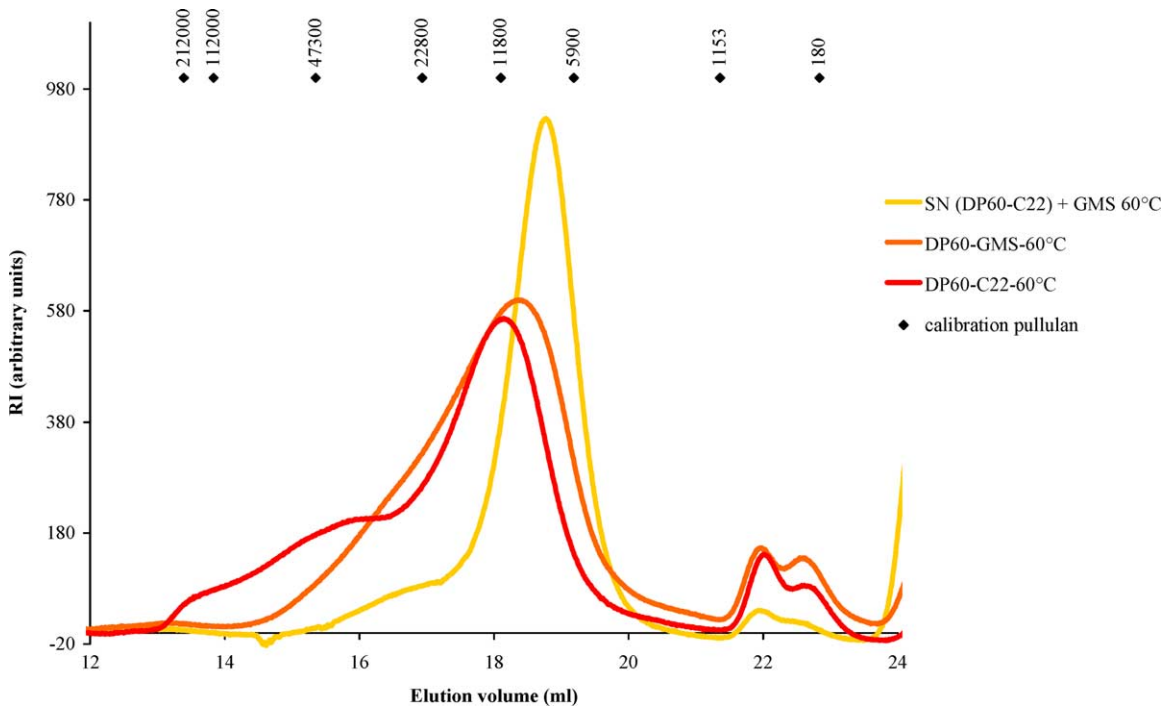

Fig. 5. Superose 12TM size-exclusion chromatogram of DP60-GMS-60 °C, DP60-C22-60 °C and the supernatant of DP60-C22-60 °C that was complexed with GMS at 60 °C (showing the refractive index signal).

bonds as described by Rappenecker and Zugenmaier (1981). Whittam et al. (1989) made a same argumentation. Discrepancies in the different studies can be attributed to different ways of evaluating the transition endotherm in the DSC thermogram, to the composition of the complex and to its preparation (Eliasson, 1994). For instance, Karkalas et al. (1995) expressed ΔH as 'J/g of amylose' rather than as 'J/g of complex', to account for possible variations in the lipid content. In analogy with Karkalas et al. (1995), the present positive relation between ΔH values and amylose DPs can be rationalised on the basis of increasing van der Waals contacts and interhelical hydrogen bonds that have to be ruptured in the larger crystals. Earlier, Godet, Buléon, Tran, and Colonna (1993b) stated that melting ΔH can be connected to the quality of the amylose packing in the complexes and that high DP amyloses can yield longer crystals. We therefore believe that the longer the amylose DP, the greater the stability and level of organization of the resulting complexes, as expressed by the increase in T_m, ΔH and relative crystallinity (see Section 3.2). However, for the longest amylose fraction (DP950), conformational disorders resulting in crystal defaults are more plausible, and may result in lower relative crystallinity and thermal stability.

3.4. Molecular weight distribution

We visualized the different amyloses and their complexes by HPAEC-PAD (Fig. 3) and by SEC (Fig. 4). Fig. 3a presents the DP20 fraction [profile (i)] and the corresponding complexes with GMS [profile (ii)] and C22 [profile (iii)] formed at 90 °C. Complexes formed at 60 °C resulted in similar profiles (not shown). A DP of 30–34 is required to complex with GMS as hardly any shorter dextrins were found in the complex profile [profile (ii)]. The peak DP of the complex 'bump' corresponds to a DP of 45. Likewise, a minimal amylose DP necessary to complex with C22 of 40 can be deduced and the peak DP of the DP20-C22-90 °C 'bump' was about 54 [profile (iii)]. This shift to higher molecular weight was expected as a longer amylose helix is required to surround C22. These data also confirm our assumptions about lower CY for low DP amyloses and the lower CY for C22- than for GMS-complexes. The chromatograms clearly evidence that the critical chain length for complex formation and precipitation corresponds to the length of two GMS or C22 molecules (see Section 3.1), as speculated earlier by Godet et al. (1995a). Dextrins of DP17 or 20, the number of glucose moieties necessary to surround one GMS or C22-molecule, respectively, are hardly detected in the DP20-complexes. Fig. 3b represents similar HPAEC-PAD profiles for DP60 [profile (i)] and its complexes formed at 90 °C [profiles (ii) and (iii)]. The supernatant, comprising all the dextrins that remained in solution during the complexation procedure of DP60-GMS-90 °C complex was analysed as well [profile (iv)]. Only dextrins with DP lower than 35 were detected, again indicating that dextrins with DP $>$ 34 form complexes and precipitate. Small variations in retention time in Fig. 3b are due to different batches of eluents.

SEC profiles of the same complexes formed at 60 and at 90 °C, presented in Fig. 4, were in line with the HPAEC-PAD results. Complexes formed at 60 or at 90 °C result in similar profiles, while the lipid type (GMS or C22) is responsible for the main differences. A dextrin population was lifted from the DP20 fraction by GMS (peak DP46) (Fig. 4a) while C22-complexes shifted to higher molecular weight (peak DP56), in agreement with HPAEC-PAD data. The high molecular weight dextrins (elution volume of 13 ml) present in the DP20 starting material were concentrated in the complexes. This fraction was probably uncompletely debranched material as already seen in Fig. 1. Size-exclusion chromatograms of DP60 and its complexes (Fig. 4b) equally demonstrated that C22-complexes have the highest molecular weight and that larger dextrins are required to complex with C22. Furthermore, Table 4 presents DP_w, DP_n and P of each amylose and the corresponding complexes. Complexation with lipids results in a P decrease. The high P value for the DP20 amylose is caused by the presence of high molecular weight dextrins as mentioned above. Without this high molecular weight fraction the P value would be 1.6 and 1.4 for the DP20 amylose and all its complexes, respectively. The chromatograms and Table 4 indicate that complexation with lipids can be exploited in fractionation procedures aiming at the recovery of specific amylose fractions with lower P. By adding a well-chosen lipid, dextrins can be separated in two fractions with a predictable critical DP. Dextrins, long enough to form a complex with the lipid will precipitate, while the shorter dextrins will remain in solution. Such fractionation is not very dependent on temperature since, in the present work, the complexation temperature only determined the quality of amylose packing (amorphous or semi-crystalline) and not the size. In contrast, fractionation of dextrin mixtures with organic solvents highly depends on temperature and time (Gelders et al., 2003). Fig. 5 clearly demonstrates these new fractionation possibilities where DP60 was complexed with C22 at 60 °C, the supernatant (dextrins with DP $<$40) was reheated to 100 °C (30 min) and equilibrated at 60 °C, then GMS was added to precipitate all dextrins with DP $>$30. SEC (Superose 12TM column) revealed a very narrow molecular weight distribution for this fraction with DP_n 46.1 and P 1.2.

4. Conclusions

CYs, relative crystallinities, T_m and ΔH increased with amylose DP (DP20–DP60–DP400) for GMS- and C22-complexes formed at 60 and at 90 °C. Conformational disorders, resulting in crystal defaults, occurred more easily with the highest DP amylose (DP950) and explain the lower relative crystallinity and thermal stability. We suggest that

an amylose DP exceeding 60 is required to yield type II complexes. Irrespective to the complexation temperature, a critical DP of 35 and 40 is necessary to complex GMS and C22, respectively. This corresponds to the length to accommodate two GMS- or C22-molecules within an amylose helix. Complexation with lipids reduces the polydispersity of the population recovered as either complex or as uncomplexed fraction. Therefore, it can be used as a new fractionation tool where successive complexation and precipitation with different lipids opens new perspectives towards nearly monodisperse amylose fractions. In further research, susceptibility of these complexes towards enzymic and acidic hydrolysis will be investigated.

Acknowledgements

Amylum Europe N.V. (Aalst, Belgium), in particular Dr A. Vidts, is gratefully acknowledged for supplying the DP20 amylose fraction and for partial funding of this work. Prof. H. Reynaers and Dr B. Goderis (Laboratory of Macromolecular Structural Chemistry, K.U. Leuven, Leuven, Belgium) are thanked for access to X-ray infrastructure and technical assistance. We thank the Fund for Scientific Research—Flanders (Fonds voor Wetenschappelijk Onderzoek—Vlaanderen) for financing the Research Assistantship of G.G. Gelders.

References

Andersson, L., Rydberg, U., Larsson, H., Andersson, R., & Åman, P. (2002). Preparation and characterisation of linear dextrins and their use as substrates in in vitro studies of starch branching enzymes. *Carbohydrate Polymers*, *47*, 53–58.

Biliaderis, C. G., & Galloway, G. (1989). Crystallization behavior of amylose-V complexes: Structure–property relationships. *Carbohydrate Research*, *189*, 31–48.

Biliaderis, C. G., & Seneviratne, H. D. (1990). On the supermolecular structure and metastability of glycerol monostearate–amylose complex. *Carbohydrate Polymers*, *13*, 185–206.

Buléon, A., Colonna, P., Planchot, V., & Ball, S. (1998). Mini review. Starch granules: Structure and biosynthesis. *International Journal of Biological Macromolecules*, *23*, 85–112.

Carlson, T. L.-G., Larsson, K., Dinh-Nguyen, N., & Krog, N. (1979). A study of the amylose–monoglyceride complex by Raman spectroscopy. *Starch/Stärke*, *31*(7), 222–224.

D'Hulst, A., & Verbeke, N. (1996). Chiral analysis of basic drugs by oligosaccharide-mediated capillary electrophoresis. *Journal of Chromatography A*, *735*, 283–293.

Eerlingen, R. C., Deceuninck, M., & Delcour, J. A. (1993). Enzyme-resistant starch. II. Influence of amylose chain length on resistant starch formation. *Cereal Chemistry*, *70*(3), 345–350.

Eliasson, A.-C. (1994). Interactions between starch and lipids studied by DSC. *Thermochimica Acta*, *246*, 343–356.

Englyst, H. N., & Cummings, J. H. (1984). Simplified method for the measurement of total non-starch polysaccharides by gas–liquid chromatography of constituent sugars as alditol acetates. *Analyst*, *109*, 937–942.

Fanta, G. F., Shogren, R. L., & Salch, J. H. (1999). Steam jet cooking of high-amylose starch–fatty acid mixtures. An investigation of complex formation. *Carbohydrate Polymers*, *38*, 1–6.

Galloway, G. I., Biliaderis, C. G., & Stanley, D. W. (1989). Properties and structure of amylose–glyceryl monostearate complexes formed in solution or on extrusion of wheat flour. *Journal of Food Science*, *54*(4), 950–957.

Gelders, G. G., Bijnens, L., Loosveld, A.-M., Vidts, A., & Delcour, J. A. (2003). Fractionation of starch hydrolysates into dextrins with narrow molecular weight distribution and their detection by high-performance anion-exchange chromatography with pulsed amperometric detection. *Journal of Chromatography A*, *992*, 75–83.

Godet, M. C., Tran, V., Delage, M. M., & Buléon, A. (1993a). Molecular modelling of the specific interactions involved in the amylose complexation by fatty acids. *International Journal of Biological Macromolecules*, *15*, 11–16.

Godet, M. C., Buléon, A., Tran, V., & Colonna, P. (1993b). Structural features of fatty acids–amylose complexes. *Carbohydrate Polymers*, *21*, 91–95.

Godet, M. C., Bizot, H., & Buléon, A. (1995a). Crystallization of amylose–fatty acid complexes prepared with different amylose chain lengths. *Carbohydrate Polymers*, *27*, 47–52.

Godet, M. C., Tran, V., Colonna, P., Buléon, A., & Pezolet, M. (1995b). Inclusion/exclusion of fatty acids in amylose complexes as a function of the fatty acid chain length. *International Journal of Biological Macromolecules*, *17*, 405–408.

Godet, M. C., Bouchet, B., Colonna, P., Gallant, D. J., & Buléon, A. (1996). Crystalline amylose–fatty acid complexes: Morphology and crystal thickness. *Journal of Food Science*, *61*(6), 1196–1201.

Hayashibare Company (1970). *Werkwijze voor de bereiding van amylose-poeder*. Octrooiraad Nederland, Nr 7001026, 198, Shimoiishi, Okayama-shi, Okayama, Japan.

Immel, S., & Lichtenthaler, F. W. (2000). The hydrophobic topographies of amylose and its blue iodine complex. *Starch/Stärke*, *52*(1), 1–8.

Karkalas, J., Ma, S., Morrison, W. R., & Pethrik, R. A. (1995). Some factors determining thermal properties of amylose inclusion complexes with fatty acids. *Carbohydrate Research*, *268*, 233–247.

Karkalas, J., & Raphaelides, S. (1986). Quantitative aspects of amylose–lipid interactions. *Carbohydrate Research*, *157*, 215–234.

Kowblansky, M. (1985). Calorimetric investigation of inclusion complexes of amylose with long-chain aliphatic compounds containing different functional groups. *Macromolecules*, *18*, 1776–1779.

Krog, N. (1971). Amylose complexing effect of food grade emulsifiers. *Starch/Stärke*, *23*(6), 206–209.

Kubik, S., & Wulff, G. (1993). Characterization and chemical modification of amylose complexes. *Starch/Stärke*, *45*(6), 220–225.

Lii, C.-Y., Stobinski, L., Tomasik, P., & Liao, C.-D. (2003). Single-walled carbon nanotube-potato amylose complex. *Carbohydrate Polymers*, *51*, 93–98.

Morrison, W. R., Tester, R. F., Snape, C. E., Law, R., & Gidley, M. J. (1993). Swelling and gelatinization of cereal starches. IV. Some effects of lipid-complexed amylose and free amylose in waxy and normal barley starches. *Cereal Chemistry*, *70*(4), 385–391.

Nuessli, J., Putaux, J. L., Le Bail, P., & Buléon, A. (2003). Crystal structure of amylose complexes with small ligands. *International Journal of Biological Macromolecules*, *33*, 227–234.

Raphaelides, S., & Karkalas, J. (1988). Thermal dissociation of amylose–fatty acid complexes. *Carbohydrate Research*, *172*, 65–82.

Rappenecker, G., & Zugenmaier, P. (1981). Detailed refinement of the crystal structure of V_h-amylose. *Carbohydrate Research*, *89*, 11–19.

Riisom, T., Krog, N., & Eriksen, J. (1984). Amylose complexing capacities of cis- and trans-unsaturated monoglycerides in relation to their functionality in bread. *Journal of Cereal Science*, *2*, 105–118.

Roger, P., Axelos, M. A. V., & Colonna, P. (2000). SEC-MALLS and SANS studies applied to solution behavior of linear alpha-glucans. *Macromolecules*, *33*, 2446–2455.

Rutschmann, M. A., & Solms, J. (1990). Formation of inclusion complexes of starch with different organic compounds. IV. Ligand binding and variability in helical conformations of V amylose complexes. *Lebensmittel-Wissenschaft und Technologie-Food Science and Technology*, *23*, 84–87.

Seneviratne, H. D., & Biliaderis, C. G. (1991). Action of alpha-amylases on amylose–lipid complex superstructures. *Journal of Cereal Science*, *13*, 129–143.

Snape, C. E., Morrison, W. R., Maroto-Valer, M. M., Karkalas, J., & Pethrick, R. A. (1998). Solid state ^{13}C NMR investigation of lipid ligands in V-amylose inclusion complexes. *Carbohydrate Polymers*, *36*, 225–237.

Star, A., Steuerman, D. W., Heath, J. R., & Stoddart, J. F. (2002). Starched carbon nanotubes. *Angewandte Chemie-International Edition*, *41*(14), 2508–2512.

Sundari, C. S., Raman, B., & Balasubramanian, D. (1999). Artificial chaperoning of insulin, human carbonic anhydrase and hen egg lysozyme using linear dextrin chains: A sweet route to the native state of globular proteins. *FEBS Letters*, *443*, 215–219.

Takeo, K., Tokumura, A., & Kuge, T. (1973). Complexes of starch and its related materials with organic compounds. Part X. X-ray diffraction of amylose–fatty acid complexes. *Starch/Stärke*, *25*(11), 357–388.

Whittam, M. A., Orford, P. D., Ring, S. G., Clark, S. A., Parker, M. L., Cairns, P., & Miles, M. J. (1989). Aqueous dissolution of crystalline and amorphous amylose–alcohol complexes. *International Journal of Biological Macromolecules*, *11*, 339–344.

Zobel, H. F. (1988). Molecules to granules: A comprehensive starch review. *Starch/Stärke*, *40*(2), 44–50.